

Nanoscale icosahedral quasicrystalline phase formation in a rapidly solidified Zr₈₀Pt₂₀ binary alloy

著者	才田 淳治
journal or publication title	Applied Physics Letters
volume	77
number	1
page range	73-75
year	2000
URL	http://hdl.handle.net/10097/47493

doi: 10.1063/1.126881

Nanoscale icosahedral quasicrystalline phase formation in a rapidly solidified $Zr_{80}Pt_{20}$ binary alloy

Junji Saida^{a)} and Mitsuhide Matsushita

Inoue Superliquid Glass Project, ERATO, Japan Science and Technology Corporation (JST), Sendai 982-0807, Japan

Akihisa Inoue

Institute for Materials Research, Tohoku University, Sendai 980-8577, Japan

(Received 10 April 2000; accepted for publication 10 May 2000)

It is found that an icosahedral quasicrystalline phase is directly formed in a $Zr_{80}Pt_{20}$ binary alloy during rapid solidification from the melt. The size of the icosahedral particles lies in the diameter range below 10 nm, and the particles are distributed homogeneously. The formation of the nanoscale icosahedral phase indicates that the icosahedral short-range order exists in the melted state of Zr–Pt binary alloy. The strong chemical affinity between Zr and Pt contributes to the restraint of the long-range rearrangement of constitutional elements to form a stable crystalline phase, which is the important factor of the stabilization of an icosahedral phase. © 2000 American Institute of Physics. [S0003-6951(00)05027-0]

Recently, the reproducible formation of an icosahedral quasicrystalline phase as a primary precipitation phase from an amorphous state has been reported over a wide annealing temperature range in the Zr–Al–Ni–Cu–M,^{1,2} Zr–Al–Ni–M,³ Zr–Ni–M⁴ (M=Ag, Pd, Au, or Pt), and Zr–TM–Pd⁵ (TM=Fe, Ni, Co, or Cu) glassy alloys. It gives a unique opportunity to clarify the kinetics^{6,7} and mechanism for the transformation from amorphous to icosahedral phase and the structural correlation⁸ between the amorphous and icosahedral phases. These results suggest that the two kinds of atomic pairs of Zr–TM and Zr–M with strongly negative heats of mixing contribute to the stabilization of glassy state and the formation of icosahedral phase through the restraint of the long-range rearrangement of constitutional atoms. Very recently, we have found the formation of icosahedral phase as a primary phase through the crystallization even in the Zr–Pd binary glassy alloy.⁹ It is implied that the Zr–M pair is a dominant factor for the formation of icosahedral phase and the Zr–TM pair stabilizes the icosahedral phase. These results also suggested that icosahedral short-range order exists in the liquid state of Zr–noble metal-based alloys. However, all the icosahedral phases are formed as a primary phase from the glassy state in these alloy systems. This letter is intended to present the direct formation of the icosahedral phase in the $Zr_{80}Pt_{20}$ binary alloy during rapid solidification from the melt.

The ribbon sample with a cross section of $0.03 \times 1 \text{ mm}^2$ was produced by melt spinning from a $Zr_{80}Pt_{20}$ arc-melted alloy ingot in an argon atmosphere. Thermal properties were measured by DSC at a heating rate of 0.67 K s^{-1} . The structure of the as-quenched sample was examined by x-ray diffractometry with Cu $K\alpha$ radiation and field-emission transmission electron microscopy (TEM) with accelerating voltage of 300 kV (JEOL JEM-3000F). The

structure of the annealed sample was also examined by x-ray diffractometry.

The oxygen content of the as-quenched $Zr_{80}Pt_{20}$ ribbon is ~ 700 ppm mass %, where the influence of oxygen impurity on the transformation behavior can be ignored.¹⁰ Figure 1 shows an x-ray diffraction (XRD) pattern of the as-quenched sample. All the diffraction peaks can be identified as the icosahedral phase. No extra peaks corresponding to the crystalline phase are seen. The bright-field TEM image (a), selected-area electron diffraction (b), and nanobeam electron diffraction patterns (c)–(e) of the as-quenched $Zr_{80}Pt_{20}$ alloy are shown in Fig. 2. Very fine particles in the diameter range below 10 nm are seen over the whole area. The precipitates have a nearly spherical morphology and are homogeneously distributed. The selected-area electron diffraction pattern taken from a region of $1 \mu\text{m}$ in diameter is observed as broad rings revealing the fine grain size. In order to confirm the structure of precipitated particles, we obtained nanobeam electron diffraction patterns of the particles with a beam di-

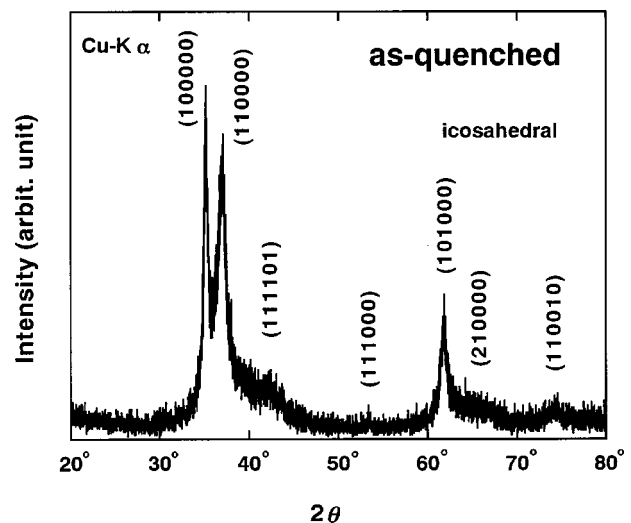


FIG. 1. X-ray diffraction pattern of the rapidly solidified $Zr_{80}Pt_{20}$ alloy.

^{a)}Electronic mail: jsaida@sendai.jst.go.jp

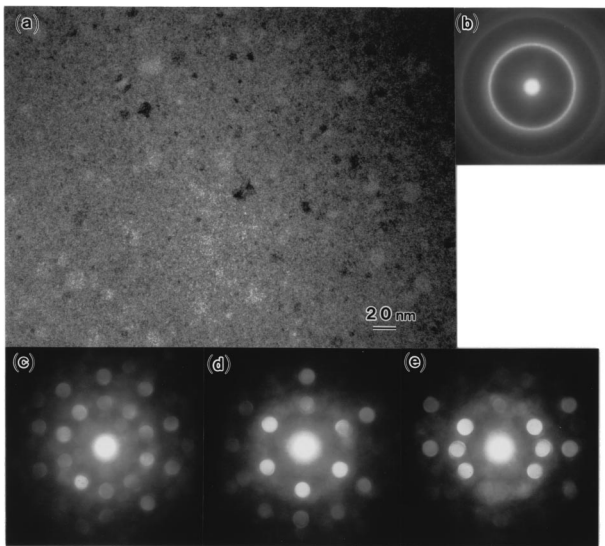


FIG. 2. Bright-field TEM image (a), selected-area electron diffraction pattern (b) and nanobeam electron diffraction patterns (c)–(e) of the rapidly solidified $Zr_{80}Pt_{20}$ alloy. The beam diameter for electron diffraction is $\sim 1 \mu\text{m}$ in (b) and is 2.4 nm in (c)–(e).

ameter of 2.4 nm. The three kinds of electron diffraction patterns reveal the five-, three- and twofold symmetries, which can be identified as the icosahedral structure. Furthermore, no extra reflection spots corresponding to a crystalline phase are seen. Thus, it is found that the icosahedral single phase is directly formed in the rapidly solidified $Zr_{80}Pt_{20}$ binary alloy. The size of the icosahedral phase is below 10 nm, being considerably smaller than that (about 20 nm) transformed from the $Zr_{70}Ni_{10}Pt_{20}$ glassy alloy.⁴

We also examined the thermal stability of the icosahedral phase. Figure 3 shows a DSC curve of the melt-spun $Zr_{80}Pt_{20}$ alloy. A single exothermic peak is observed and the onset temperature, T_x of the exothermic peak is 895 K, implying that the exothermic reaction corresponds to a transformation from icosahedral to crystalline phase. Figure 4 shows an x-ray diffraction pattern of the $Zr_{80}Pt_{20}$ alloy annealed for 3.6 ks at 1000 K. The diffraction peaks are identified as Zr, ZrPt, and Zr_3Pt_5 phases. Since neither diffraction peaks of icosahedral phase nor broad peak due to the amorphous phase are recognized, the icosahedral phase obtained in the

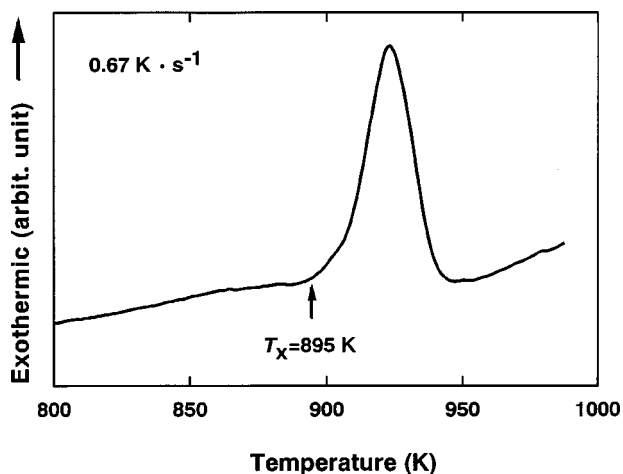


FIG. 3. DSC curve of the rapidly solidified $Zr_{80}Pt_{20}$ alloy. Downloaded 14 Feb 2010 to 130.34.135.83. Redistribution subject to

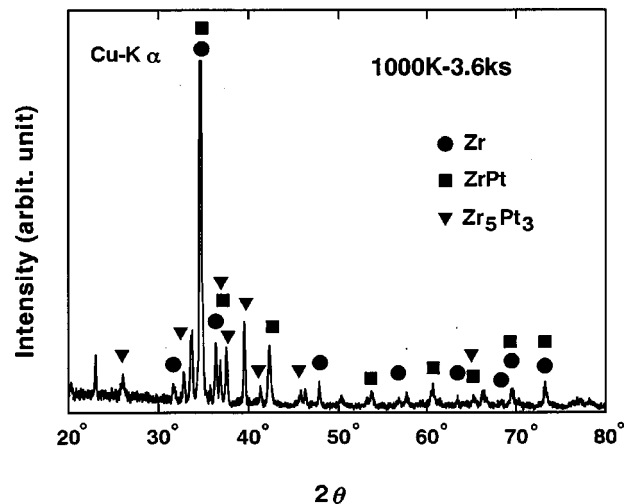


FIG. 4. X-ray diffraction pattern of the $Zr_{80}Pt_{20}$ melt-spun ribbon annealed for 3.6 ks at 1000 K.

melt-spun alloy is a metastable phase. The exothermic peak is, therefore concluded to result from the transition from the icosahedral phase to the stable crystalline phases of Zr, ZrPt, and Zr_3Pt_5 . The onset temperature of the exothermic peak is considerably higher than that of the transformation from icosahedral phase to crystalline phase (~ 845 K) for the $Zr_{70}Ni_{10}Pt_{20}$ alloy, implying the higher thermal stability of the icosahedral phase in the melt-spun $Zr_{80}Pt_{20}$ alloy.

We have previously reported the formation of the icosahedral phase in the Zr–Ni–M (M=Pd, Au or Pt) and Zr–TM–Pd (TM=Fe, Ni, Co, or Cu) ternary systems.^{4,5} In these icosahedral alloys, one has pointed out the correlation between the existence of an icosahedral short-range order^{11,12} and atomic configurations due to the chemical affinity of constitutional elements. Very recently, it has been found that the icosahedral phase is formed even in the Zr–Pd binary glassy alloy,⁹ suggesting the structural correlation between the icosahedral phase and the short-range ordering in the glassy state under the only strong chemical pair of Zr–Pd. The heat of mixing for Zr–Pt atomic pair also has an extremely large negative value of -376 kJ mol^{-1} .¹³ The formation of the icosahedral phase in the melt-spun Zr–Pt binary alloy indicates that an icosahedral short-range order exists in the liquid state and the strong atomic pair suppresses the long-range rearrangement of atoms to form the stable crystalline phase, leading to the stability of the icosahedral short-range order. The precipitation of nanoscale icosahedral particles also reflects the stability of the icosahedral short-range order and difficulty of the long-range rearrangement for grain growth through the crystallization. Thus, the icosahedral short-range order is expected to be stable in the Zr-noble metal-based alloys, which is an important factor for the appearance of the supercooled liquid state in the alloys.

The nanoscale icosahedral phase was found to be formed in the rapidly solidified $Zr_{80}Pt_{20}$ binary alloy. The icosahedral particles have a nearly spherical morphology with a diameter range below 10 nm. The icosahedral phase has a high thermal stability and transforms to the crystalline Zr, ZrPt, and Zr_3Pt_5 phases at 895 K at the heating rate of 0.67 k s^{-1} . The direct formation of the icosahedral phase from the liquid AIP license or copyright; see <http://apl.aip.org/apl/copyright.jsp>

phase suggests that an icosahedral short-range order exists in the melt of Zr–Pt binary alloy and the long-range atomic rearrangements for the transition from the icosahedral order to the periodic order is suppressed by the strong chemical affinity between Zr and Pt.

¹M. W. Chen, T. Zhang, A. Inoue, A. Sakai, and T. Sakurai, *Appl. Phys. Lett.* **75**, 1697 (1999).

²A. Inoue, T. Zhang, J. Saida, M. Matsushita, M. W. Chen, and T. Sakurai, *Mater. Trans., JIM* **40**, 1181 (1999).

³A. Inoue, J. Saida, M. Matsushita, and T. Sakurai, *Mater. Trans., JIM* **41**, 362 (2000).

⁴J. Saida, M. Matsushita, C. Li, and A. Inoue, *Appl. Phys. Lett.* (in press).

⁵M. Matsushita, J. Saida, C. Li, and A. Inoue, *J. Mater. Res.* (in press).

⁶J. Saida, M. Matsushita, T. Zhang, A. Inoue, M. W. Chen, and T. Sakurai, *Appl. Phys. Lett.* **75**, 3497 (1999).

⁷M. Matsushita, J. Saida, T. Zhang, A. Inoue, M. W. Chen, and T. Sakurai, *Philos. Mag. Lett.* **80**, 79 (2000).

⁸L. C. Chen and F. Spaepen, *Nature (London)* **336**, 366 (1988).

⁹J. Saida, M. Matsushita, C. Li, and A. Inoue, *Philos. Mag. Lett.* (accepted for publication).

¹⁰B. S. Murty, D. H. Ping, K. Hono, and A. Inoue, *Appl. Phys. Lett.* **76**, 55 (2000).

¹¹Y. Shen, S. J. Poon, and G. J. Shiflet, *Phys. Rev. B* **34**, 3516 (1986).

¹²E. Matsubara, Y. Waseda, A. P. Tsai, A. Inoue, and T. Masumoto, *J. Mater. Sci.* **25**, 2507 (1990).

¹³A. K. Niessen, F. R. de Bore, S. Boom, P. F. de Châtel, W. C. M. Mattens, and A. R. Miedema, *CALPHAD: Comput. Coupling Phase Diagrams Thermochem.* **7**, 51 (1983).